

## **Numerical study of optical performance of a parabolic-trough concentrating solar power system**

\*Raquel Miguez de Carvalho<sup>1)</sup>, Mavd R. Teles<sup>2)</sup> and Kamal A. R. Ismail<sup>3)</sup>

<sup>1), 2), 3)</sup> *Department of Energy, Faculty of Mechanical Engineering, State University of Campinas, Campinas, Brazil*

<sup>1)</sup> [raquel.miguezcarvalho@gmail.com.br](mailto:raquel.miguezcarvalho@gmail.com.br) <sup>3)</sup> [kamal@fem.unicamp.br](mailto:kamal@fem.unicamp.br)

### **ABSTRACT**

The global increase in energy demands due to growth of world population, expansion of industrial activities, progress and development in developing countries associated with the alarming increase in greenhouse gases (GHG) alerted the world about the eminent risks of the present environment scenario and its disastrous implications. This led to enhance research and development activities to supplement and possibly substitute the world present and future energy sources with renewable and sustainable sources. Solar energy occupies the top of the list of most viable sources with relatively well dominated technologies and extensive field of applications ranging from low to high temperature as well as direct energy conversion to electricity. Cooling usually consumes a lot of energy and represents an essential field of activities of vital interest to the society. Solar energy can be harnessed by using some special solar collectors to provide electricity directly and/or hot fluids at relatively high temperatures such as parabolic-trough concentrating (PTC) systems to provide electricity by thermal machines. This paper analyses the geometry influence on the optical performance of some designs for this type of collectors for use in absorption refrigeration system for a small installation as a residence. The present paper also presents a numerical study of the local concentration ratio (LCR) based on the Monte Carlo Ray Tracing (MCRT) method. In this study the slope and orientation of one-axis tracking system, the ratio of the beam radiation on a slope plane to the horizontal and the ratio of hourly to daily diffuse solar radiation is determined.

**Keywords:** solar energy, renewable energy, parabolic-trough concentrating, optical performance, numerical analysis, solar radiation.

---

<sup>1)</sup> Corresponding author, master's student.

<sup>2)</sup> Master's student

<sup>3)</sup> Full Professor.

## **1. INTRODUCTION**

The conventional energy sources have harmful environmental impacts as GHG emission. Kalogirou (2004) discusses how renewable energy systems can have beneficial impacts on the environment by decreasing environmental pollution and GHG emissions, economic impact by creating jobs and income, conservation of natural resources especially water and energy and most important of all national accessibility.

Solar energy systems can generate thermal and electrical energy from solar radiation. Duffie (2013) describes a solar collector as a special kind of heat exchanger that collect the radiation heat from the sun and transforms into internal energy of the working fluid. Different solar collector types produce different temperature levels. Cooling usually consumes a lot of energy, one way to increase the absorbed amount of energy is to reduce heat losses from the absorber decreasing its area and keeping the heat gain. This can be done by adding an optical device between the source of radiation and the absorber. This optical device is a concentrator, it usually has concave reflecting surface to intercept and focus the sun's radiation beam on the absorber.

Kalogirou (2004) presents various types of solar thermal collectors. Conventional concentrating collectors must follow the apparent movement of the sun across the sky. There are two tracking methods, the first is the altazimuth which enables the concentrator to follow the sun exactly. The second is the one-axis tracking in which the collector tracks the sun in only one direction either from east to west or from north to south.

Lovegrove (2012) explains that the position of the parabolic-trough collectors must be such that the sun vector, the collector focal line and the vector perpendicular to the collector aperture plane are in the same plane, otherwise the reflected rays are not focused to a unique focal point. For this reason, PTC requires solar tracking system. To estimate the optical performance, it is important to evaluate the geometry of the collector and possible shades during the day. Jeter (1983) analyzes the influences of three factors that reduces the effective aperture of the collector.

Jeter (1986) established the first integral of the differential energy flux density for trough concentrators, this result includes formulation of the perfect parabolic trough collectors with a flat plane and a round receiver centered on the focus. For numerical results, the MCRT is detailed by He(2011). This method combined with finite volume method is used calculated the non-uniform heat flux distribution considered as the boundary condition.

Liu (1960) presents relationships that determine statistical distribution of daily total and diffuse radiation of some localities in the United States and Canada, knowing the direct radiation, while Collares-Pereira (1979) correlates Hottel, Whillier and Liu and Jordan between the diffuse and total hourly radiation.

The present paper compares the geometrical concentration, the optical performance and the effective aperture area for different configurations of PTC with the same length and width for use in absorption refrigeration system for a small residential installation. The slope and orientation of the tracking system for each representative day of the month for the latitude of Campinas, Brazil is also presented. A two dimensional numerical approximation of the LCR based on MCRT method is used to analyze the influence of these designs on the LCR. Finally, the ratio of the beam radiation on an

inclined plane to the beam radiation on the horizontal surface is calculated for each average day of the month, and the ratio of the hourly diffuse radiation to daily diffuse radiation is also calculated for the receiver.

## 2. GEOMETRICAL CONSIDERATIONS OF THE PARABOLIC CONCENTRATOR

### 2.1 Determination of minimum absorber diameter and concentration

Concentrating collectors are composed of a receiver and a concentrator. The receiver is where the radiation is absorbed and the concentrator is the optical system, it has a bigger area than that of the receiver and direct the incidence rays of the sun that falls on the reflective surface on the absorber surface. For PTC, the concentrator has a parabolic geometry. Parallel rays that enters perpendicular to the aperture plane are directed to the focus point.

Fig. 1 shows a cross section of a linear parabolic concentrator. For both Fig. 1a and Fig. 1b, A is the center of the parabola, B is the end of the concentrator and F is the parabola's focus. Fig. 1b shows that the incident beam of solar radiation forms a cone with an angular width of  $0.53^\circ$ , this angle will be used to calculate the minimum diameter of the absorber. The present concentrator has 6 m length and 2 m width. The others parameters are calculated using Eq. 1-5 for different rim angles.

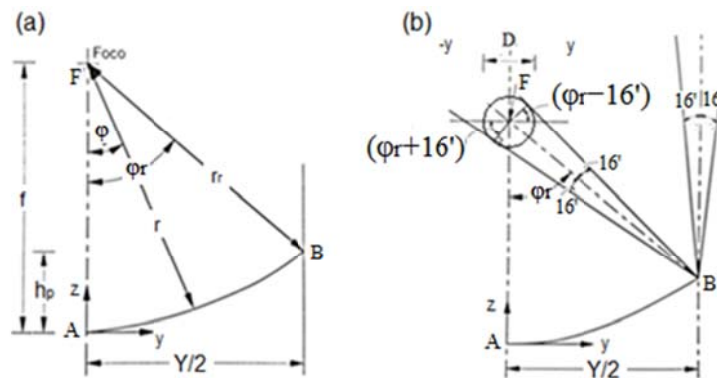


Fig. 1 Section of a linear parabolic concentrator showing major dimensions. Adapted from Duffie and Beckman (2013)

The maximum mirror radius is at the rim angle. It is the distance between point F and point B, as shown in Fig. 1 and it is calculated by Eq. (1), Lovegrove (2012):

$$r_r = \frac{Y}{2 \sin \phi_r} \quad (1)$$

Where  $Y$  is the width of the concentrator and  $\phi_r$  is the rim angle.

The focal length is the distance from the focus (point F) to the vertex (point A) of the parabola, Duffie (2013).

$$f = \frac{r_r(1 + \cos(\varphi_r))}{2} \quad (2)$$

The minimum diameter is calculated in terms of the maximum mirror radius and the optical cone of an incident beam of solar radiation, Duffie (2013).

$$D_{\min} = 2r_r \sin(0.267^\circ) \quad (3)$$

The height between the end of the concentrator and the vertex, Lovegrove (2012) is:

$$h_p = \frac{r_r^2}{4f} \quad (4)$$

The area concentration ratio is the ratio of the aperture area to the absorber area and can be calculated by Duffie (2013):

$$GC = \frac{Y}{\pi D} \quad (5)$$

The effect of varying rim angles on the minimum diameter and on the concentration is shown in Fig. 2 and 3, respectively.

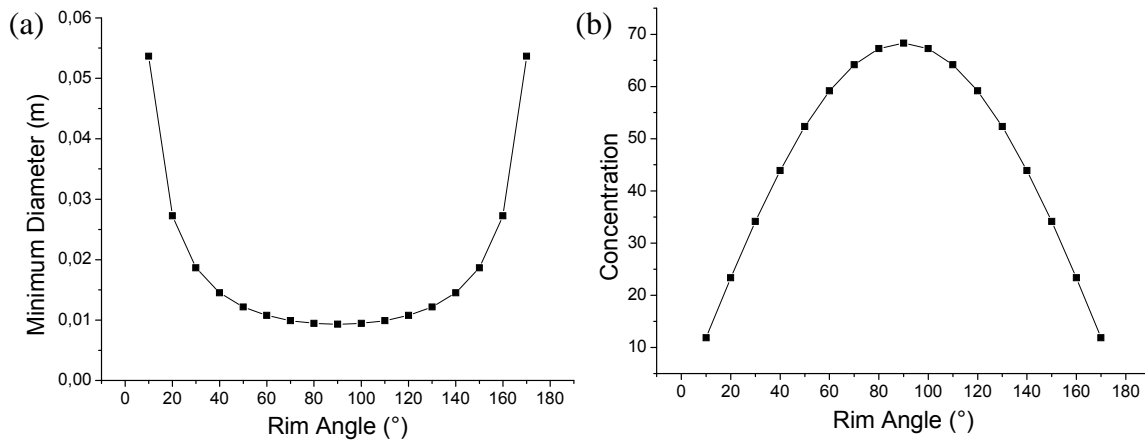


Fig. 2 The effect of varying rim angles on (a) Minimum diameter of the collector (b) Concentration of the collector

The concentration is inversely proportional to the minimum diameter. The best rim angle is 90°, because it gives the biggest concentration. On the other hand, in manufacturing the configuration uses more material thus more expensive.

The design of the concentrators for each rim angle and its corresponding focal point is shown in Fig. 3.

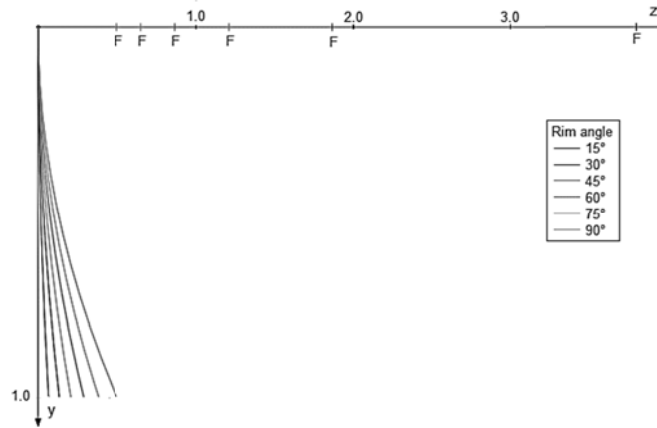


Fig. 3 Concentrator design for each rim angle.

Small rim angles do not allowed big concentration and its focal point is far from the collector, what can bring structural problems with the receiver supports.

## 2.2 Tracking System

The slope of the collector aperture plane is calculated in terms of the declination angle of the sun and the local latitude. The collector is installed in Campinas, Brazil, where the latitude is  $22^{\circ} 54' S$ . The vector perpendicular to the collector aperture plane, the sun vector and the collector focal line must be in the same plane. The declination angle of the sun varies for each day of the year.

The present collector has one-axis tracking. It rotates about the horizontal east-west axis and it requires a single daily adjustment. In this case, the beam radiation is normal to the surface at noon each day ( $\theta = 0^{\circ}$ ), Duffie (2013).

The declination angle of the sun is the angular position of the sun at noon, and a good approximation can be calculated in function of the day of the year.

$$\delta = 23,45^{\circ} \sin \left[ 360 \frac{(284 + n)}{365} \right] \quad (6)$$

For the present tracking mode, the slope is calculated as in Eq. (7):

$$\beta = |\phi - \delta| \quad (7)$$

Where  $\phi$  is the latitude.

The orientation of the collector will change between south and north depending on the azimuth angle,  $\gamma$ .

$$\left. \begin{array}{l} \gamma = 0^{\circ}(\text{South}) \\ \gamma = 180^{\circ}(\text{North}) \end{array} \right\} \begin{array}{l} \text{if } \phi - \delta > 0 \\ \text{if } \phi - \delta \leq 0 \end{array} \quad (8)$$

The results for each average day of the month are shown in Tab. 1.

Tab.1 Slope and orientation for each day for the Average Day of the Month

Day	Slope	Orientation
January 17 <sup>th</sup>	1.99°	North
February 16 <sup>th</sup>	9.95°	North
March 16 <sup>th</sup>	20.49°	North
April 15 <sup>th</sup>	32.32°	North
May 15 <sup>th</sup>	41.70°	North
June 11 <sup>th</sup>	45.99°	North
July 17 <sup>th</sup>	44.09°	North
August 16 <sup>th</sup>	36.36°	North
September 15 <sup>th</sup>	25.12°	North
October 15 <sup>th</sup>	13.31°	North
November 14 <sup>th</sup>	3.99°	North
December 10 <sup>th</sup>	0.14°	South

When the declination angle of the sun is smaller than the local latitude, the orientation of the collector changes from north to south, if it is located in south hemisphere. This occurs only in December for the average day of the month in Campinas.

### 3. DIRECT AND DIFFUSE SOLAR RADIATION

Duffie (2013) explains the kinds of solar radiation. The direct or beam radiation as the radiation that comes direct from the sun, without having been scattered by the atmosphere, the diffuse radiation is the solar radiation received from the sun after its direction has been changed by scattering by the atmosphere, and total radiation as a sum of beam and diffuse radiation on a surface.

The ratio of beam radiation on tilted surfaces to the beam radiation on horizontal surfaces,  $R_b$ , over a time period from  $w_1$  to  $w_2$  can be approximated by Duffie (2013):

$$R_b = \frac{a}{b} \quad (9)$$

Where a is:

$$a = (\sin \delta \sin \phi \cos \beta - \sin \delta \cos \phi \sin \beta \cos \gamma) \frac{\pi(w_2 - w_1)}{180} - (\cos \delta \sin \beta \sin \gamma)(\cos w_2 - \cos w_1) + (\cos \delta \cos \phi \cos \beta + \cos \delta \sin \phi \sin \beta \cos \gamma)(\sin w_2 - \sin w_1) \quad (10)$$

Where  $\delta$  is the declination angle,  $\phi$  is the latitude,  $\beta$  is the slope of the surface and  $\gamma$  is the azimuth angle.

And the value of b is given by:

$$b = (\cos \phi \cos \delta)(\sin w_2 - \sin w_1) + (\sin \phi \sin \delta) \frac{\pi(w_2 - w_1)}{180} \quad (11)$$

Fig. 4 shows the results of this ratio for the average days of the months in Campinas.

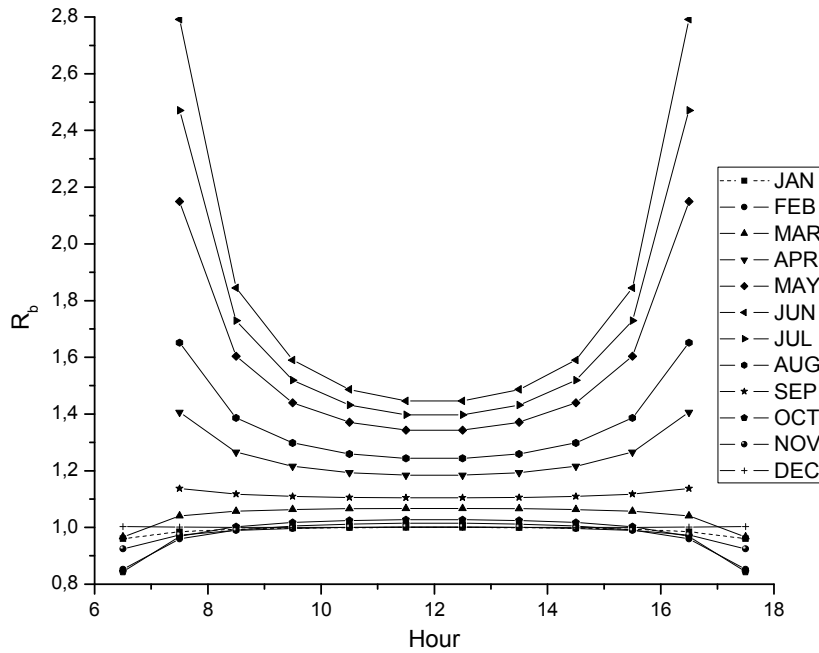


Fig. 4 Hourly ratio of beam radiation on a slope plane to the horizontal

The ratio increases in the winter months, because the slope is bigger than in the summer months.

The parabolic concentrator cannot concentrate the diffuse radiation, because it comes from different directions, but the receiver absorbs both radiations. For this reason, the ratio of the hourly diffuse radiation to the daily diffuse radiation,  $r_d$ , is calculated by:

$$r_d = \frac{\pi \cos \phi \cos \delta \cos w + \sin \phi \sin \delta}{24 \cos \phi \cos \delta \sin w_s + w_s \sin \phi \sin \delta} \quad (12)$$

Where  $w$  is the hour angle ( $15^\circ$  per hour, morning negative and afternoon positive) and  $w_s$  is the sunset hour angle and is calculated by:

$$w_s = -\tan \phi \tan \delta \quad (13)$$

The results for each average day of the month are shown in Fig. 5.

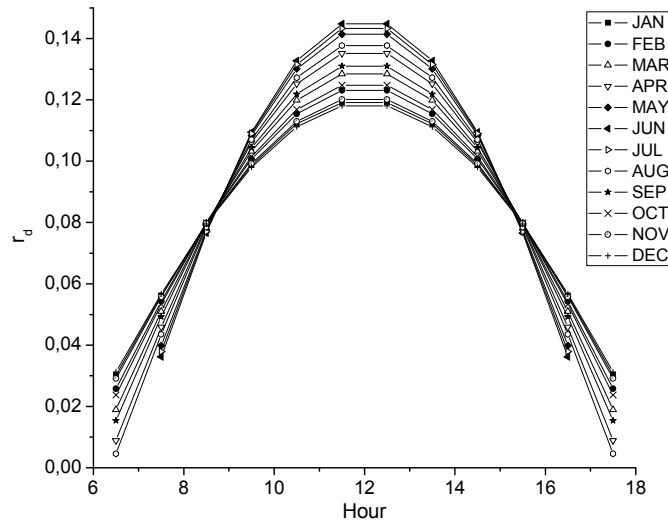


Fig. 5 Ratio of hourly diffuse radiation to daily diffuse radiation

The ratio is symmetrical at noon. In winter months, the sun rises one hour later and sets one hour earlier, as the daily diffuse radiation is divided by fewer hours, its ratio is larger than in summer months.

#### 4. OPTICAL EFFICIENCY AND GEOMETRY EFFECTS

The optical efficiency depends on the optical properties of the materials involved, the geometry of the collector and the various imperfections arising from the construction of the collector. The losses are associated with four parameters: reflectivity, intercept factor (geometrical errors collector's shape, shadowing by the flexible bellows and mechanical deformation of the support structure), transmissivity and absorptivity. Furthermore, the incidence angle of the beam solar radiation affects those four parameters; however, this effect can be quantified by the incidence angle modifier. The specifications of the collector are detailed in Tab. 2.

Tab. 2 Optical parameters

Characterization	Collector parameters
Reflector material	Aluminium
Reflectivity	0.95
Intercept factor	0.91
Transmissivity of the glass	0.92
Steel pipe coat	Cermet black chrome coating
Absorptivity	0.95

The angle between the beam radiation on a surface and the normal to that surface is called the incidence angle, and can be calculated by the following equation Duffie (2013):

$$\theta = \arccos(\sin^2(\delta) + \cos^2(\delta)\cos(w)) \quad (14)$$

Where  $w$  is the hour angle.

The optical performance at noon is calculated with Eq. (15), Lovegrove (2012):

$$\eta_{opt,0^\circ} = \rho\gamma\tau\alpha|_{\theta=0^\circ} \quad (15)$$

Where  $\rho$  is the reflectivity of the concentrator surface,  $\gamma$  is the intercept factor,  $\tau$  is the transmissivity of the glass of the external evacuated tube and  $\alpha$  is the absorptivity of the absorber.

The optical performance for the other incidence angles is calculated in function of the incidence angle modifier Lovegrove (2012).

$$\eta_{opt,\theta \neq 0^\circ} = \eta_{opt,0^\circ} K(\theta) \quad (16)$$

Where  $K(\theta)$  is the incidence angle modifier and it is calculated with Eq. (17) and (18) Lovegrove (2012):

For ( $0^\circ < \theta < 80^\circ$ ):

$$K(\theta) = 1 - 2.23073E - 4 * \theta - 1.1E - 4 * \theta^2 + 3.18596E - 6 * \theta^3 - 4.85509E - 8 * \theta^4 \quad (17)$$

For ( $85^\circ < \theta < 90^\circ$ ):

$$K(\theta) = 0 \quad (18)$$

The effect of the incidence angle on the optical efficiency is shown Fig.6.

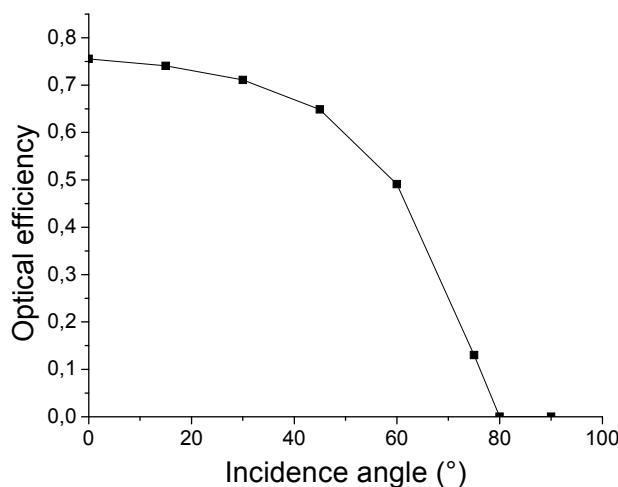


Fig. 6 Optical efficiency at different incidence angles

The polynomial of the incidence angle modifier acts up to 80°. After 85° it drops to zero, because after 85° the sun is almost set. Until  $\theta = 45^\circ$ , the efficiency decreases 10%, while there is a 15% fall between 60° and 45°, thus after 45° the decrease rate is much more.

There are three geometric factors that reduce the effective aperture area of the collector and hence affecting the optical efficiency. These factors are: the end effect (some of the rays reflected near the end of the concentrator cannot reach the receiver), shade by bulkheads and shade by neighboring collectors in an array. To avoid the shade by neighboring collectors, the minimum distance between the collectors is calculated as in Eq. (19) Jeter (1983):

$$P = \frac{Y}{\sin(90 - \beta_{\max})} \quad (19)$$

The maximum  $\beta$  is when the declination angle is 23.45°, in this case, the minimum distance between the collectors must be 2.9 m.

The other two effects are calculated to determine the effective aperture area Jeter (1983). The end effect and the shade area due to bulkheads are calculated as:

$$A_i = f * Y * \tan \theta \left( 1 + \frac{Y^2}{48f^2} \right) \quad (20)$$

$$A_b = 2 * Y * h_p * \tan \theta / 3 \quad (21)$$

The ratio of the effective aperture area to the total aperture area is:

$$A_f = \frac{A_e}{A} = \frac{A - (A_i + A_b)}{A} \quad (22)$$

Where A is the total aperture area,  $A_e$  is the effective area,  $A_i$  is the affected area by the end effect and  $A_b$  is the shade area due to bulkheads.

The effective aperture area depends on the incidence and rim angles.

Fig. 7 shows that the biggest effective aperture areas are for rim angles of 110° and 130°, but the difference between them and 90° is not very significant until the incidence angle reaches 65°. After an incidence angle of 75°, there isn't effective area anymore for the rim angle of 30°.

Finally, the total optical efficiency is a function of the optical efficiency, the incidence angle modifier and the ratio of the effective aperture area to the total aperture area Jeter (1983).

$$\eta_o = \rho \gamma \tau \alpha K(\theta) A_f \quad (23)$$

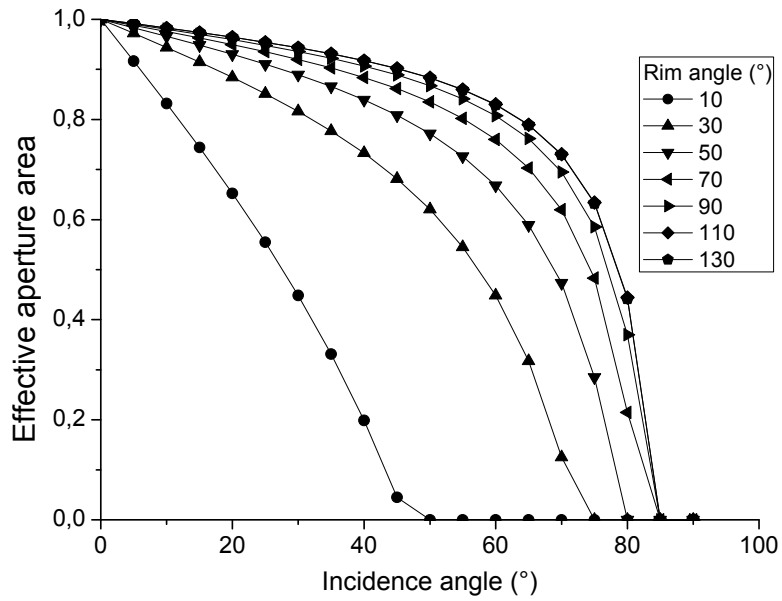


Fig.7 Effective aperture area for different rim angles at different incidence angles

For the total optical efficiency, the results of optical efficiency shown in Fig. 6 are multiplied by the effective aperture area and the results in Fig. 7 and the results are plotted in Fig. 8.

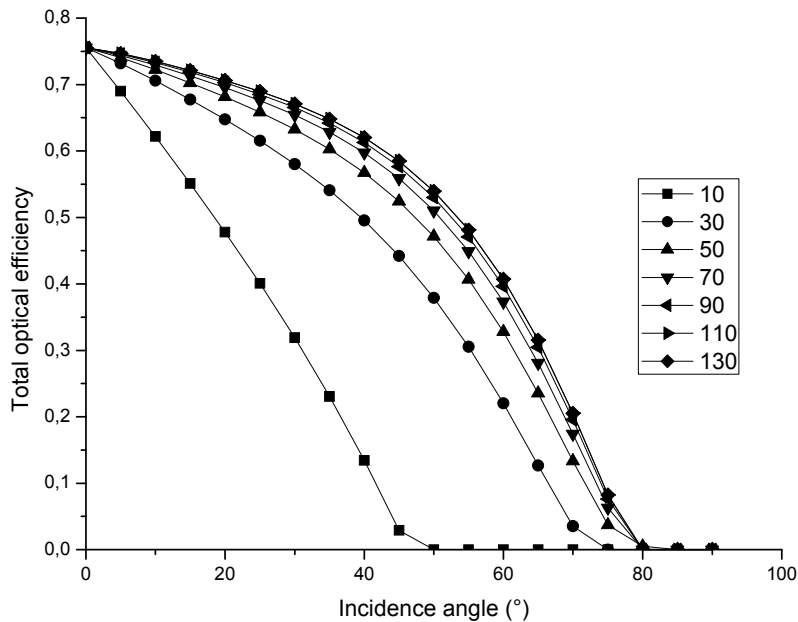


Fig. 8 Total Optical efficiency for different rim angles at different angles of incidence

The highest total optical efficiency still at rim angles of 110° and 130°, but the difference between them and 90° is smaller than the difference in Fig. 7. After 80°, there is not optical efficiency anymore, and hence there is not total optical efficiency too.

A flowchart that synthesizes the steps until this section was made for a better visualization of the present paper. Each subroutine calculate one section of the paper. Some output data of one subroutine is the input of other. The direct and diffuse solar radiation depends on the declination, the slope and the azimuth angles that have already been calculated in the section 2.2. The optical performance depends on some geometry output data of the section 2.1 and the declination of the section 2.2. This flowchart is shown in Fig. 9.

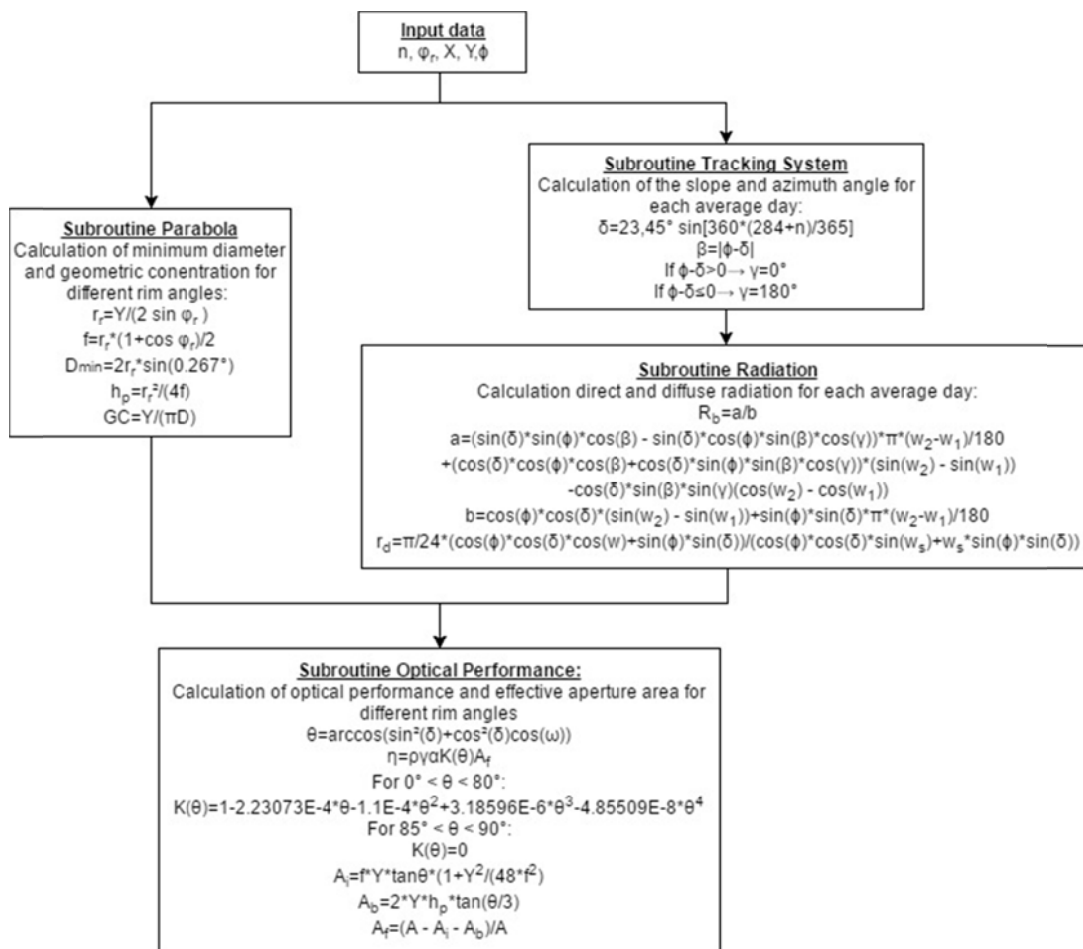


Fig. 9 Flowchart

## 5. ANALYSIS OF LOCAL CONCENTRATION RATIO OF THE RECEIVER

The Local Concentration Ratio (LCR) is the ratio of solar radiative heat flux falling on the surface of the absorber to that falling on the aperture plane of the concentrator. A two dimensional numerical program based on MCRT method is used to analyze the

influence of these configurations on the LCR. It is a statistical method and which random sunrays are generated by the computer, if the ray hit the absorber directly or if it was redirect by the parabola, the angle where it hit will be counted. Only half parabola was calculated, because it is symmetrical.

Using geometry knowledge, the equations from He (2011) are adapted for a two dimensional study by author. The number of randomly sunrays generated in this program is 25000000.

Firstly, the position of the ray in y-direction is calculated:

$$y_1 = \xi_1 \frac{Y}{2} \quad (24)$$

Where  $\xi_1$  is a random number between 0 and 1, so  $y_1$  varies between 0 and half width. If  $y_1$  is less or equal the receiver radius, then  $z_1$  is calculated by:

$$z_1 = \sqrt{r^2 - y_1^2} \quad (25)$$

Where  $r$  is the receiver radius. The angle that will be count is:

$$\beta = \arctan\left(\frac{z_1}{y_1}\right) \quad (26)$$

If  $y_1$  is greater than the receiver radius, so it falls on the receiver surface in the point  $(y_1, z_1)$ , where  $z_1$  is calculated by:

$$z_1 = \frac{y_1^2}{4f} \quad (27)$$

Where  $f$  is the focal length. The ray will be redirect if a second random number, also between 0 and 1, is less or equal the reflectivity of the concentrator surface.

A deflection angle  $\theta$  will be considerate as:

$$\theta = -\theta_{sun} + 2\xi_3\theta_{sun} \quad (28)$$

Where  $\theta_{sun}$  is  $16'$  and  $\xi_3$  is a third random number also between 0 and 1, hence  $-\theta_{sun} < \theta < \theta_{sun}$ .

When the ray hit the parabola, its direction changes. If the ray hits the receiver will be at the point  $(y_2, z_2)$  that satisfies the following system of equations:

$$\left. \begin{aligned} z_2^2 + y_2^2 &= r^2 \\ (z_2 - z_1) &= \frac{(y_2 - y_1)}{\tan(\varphi - \theta)} \end{aligned} \right\} \quad (29)$$

Where  $\varphi$  is the angle shaped by the segments between the point  $(y_1, z_1)$  and the focal point, and between the focal point and the vertex of the parabola. This root-finding problem is solved using Newton's method.

The relationship between the heat flux distribution and LCR is as in Eq. (30) He (2011):

$$q_i = LCR \cdot q_{sun} \quad (30)$$

Where  $q_i$  is the heat flux distribution on the receiver and  $q_{sun}$  is the direct normal insolation. The heat flux distribution can be also calculated by He (2011):

$$q_i = p_i \frac{q_{sun} XY}{NS_i} \quad (31)$$

Where  $p_i$  is an array used to count the rays that hit the absorber,  $X$  is the length of the parabola,  $Y$  is the width,  $N$  is the number rays that was used on the code and  $S_i$  is the area of the element that contains  $p_i$ , it depends on the number of segments the receiver is divided.

$$S_i = \frac{\pi r}{n} X \quad (32)$$

Where  $n$  is the number of segments the receiver is divided. Replacing Eq. (32) and (5) in Eq. (31), and comparing to Eq. (30), LCR can be calculated in terms of  $p_i$ .

$$LCR = \frac{p_i \cdot GC \cdot n}{N} \quad (33)$$

To verify the accuracy of the simulation, an ideal PTC with round absorber, with geometric concentration (GC) is 20, rim angle of  $90^\circ$  and  $\theta_{sun} = 0.0075$  rad that was adopted by Jeter (1986) is used and the present numerical results are compared with Jeter's analytical results and are shown in Fig. 10.

Comparing the analytical and the numerical result, the two curves follow the same trend and the values of both curves are very close, which verify that the present code is reliable.

In order to compare the LCR for different rim angles, the GC is maintained 20, with the same width of 2 m and for the configurations shown in Fig. 3, the numerical results are shown in Fig. 11.

For smaller rim angles, the LCR reaches larger numbers but concentrated in smaller areas, and for bigger rim angles, the LCR covers a larger area. The total LCR is practically the same for all angles. As the Fig. 11 shows, all curves have 4 significant parts, in the first part, the absorber shades the concentrator, hence the reflection is impaired. In the second part the concentration increases until a peak that varies for each rim angle, after this peak, the third part is a rapidly decrease and the last part is the direct radiation area.

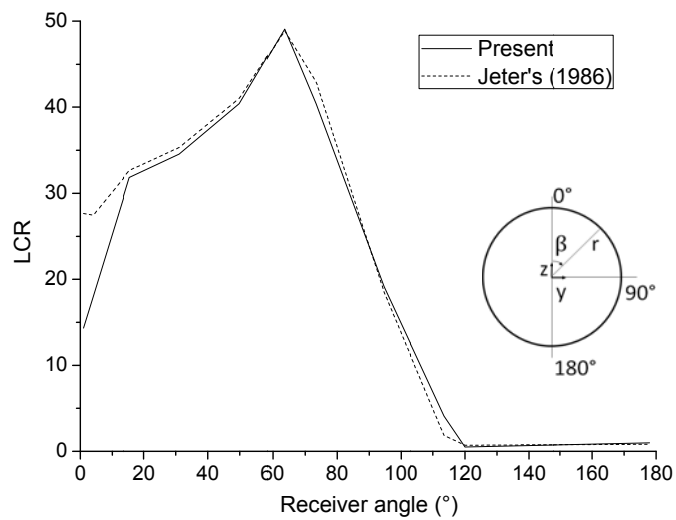


Fig. 10 Local concentration ratio distribution

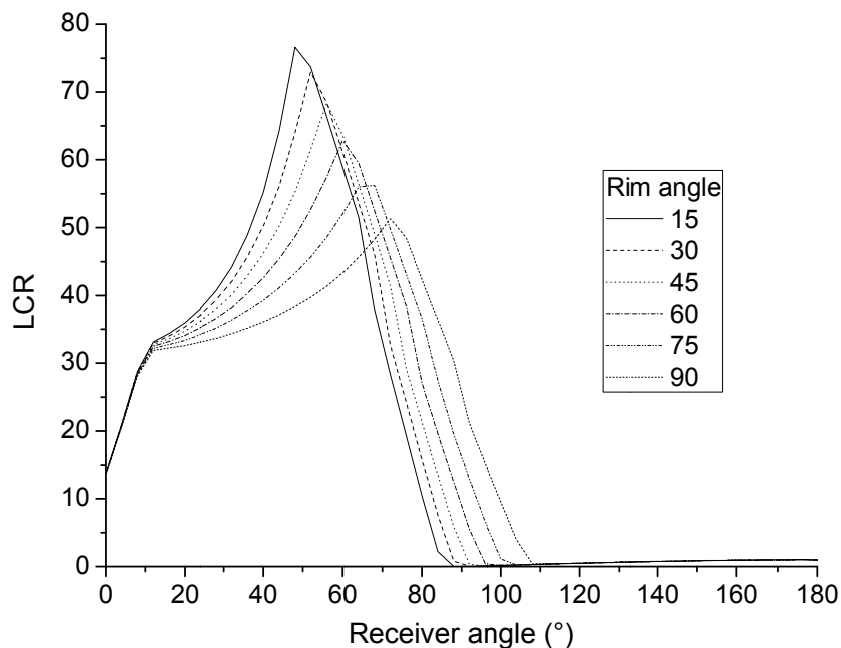


Fig. 11 Local concentration ratio distribution under different rim angles

The flowchart of the method of this section is shown in Fig. 12. Before starts, the number of segments that the absorber will be divided must to be chosen and the array that will be used to count the rays must be set out in function of that. The program generates random numbers, these numbers are used to calculated 25000000 different y positions of the sunrays. Then it calculate if each ray will hit the absorber directly, if does, where hit in polar coordinate, if doesn't, another random number is generate and if it is less or equal the reflectivity of the concentrator the program will calculate the

redirection of the ray by the concentrator surface considering the deflection angle of the sun if. Once again, the program checks if the ray will hit the absorber and if it hits it will count in polar coordinate. Finally, the program converts the array that was used to count in LCR.

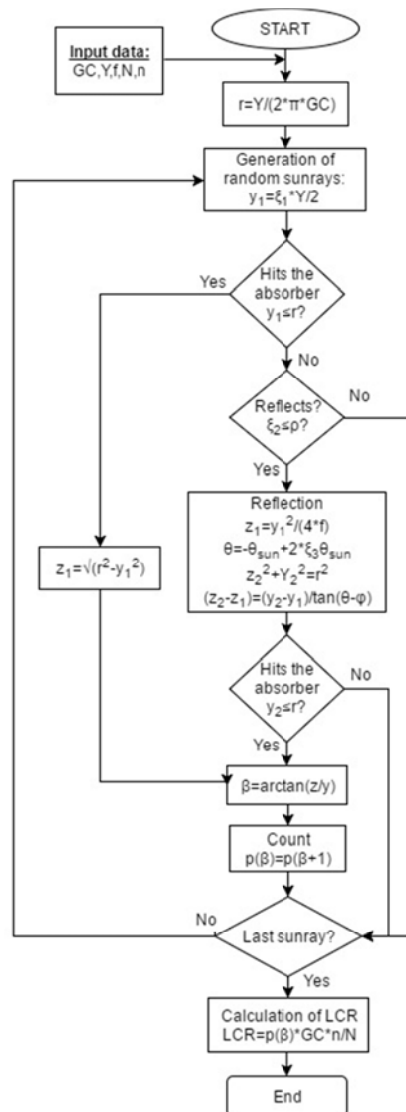


Fig. 12 Flowchart of the numerical model

## 6. CONCLUSIONS

This work analyses some of the PTC geometrical configurations and their influence on the optical performance and LCR including the influence of the locality of installation. A two dimensional numerical code based on MCRT is presented and validated against available data. The rim angle which allows the biggest concentration

is 90°. The total LCR is not affected by the rim angle, but rim angle of 90° gives more uniform concentration ratio over the absorber than other angles.

## ACKNOWLEDGMENTS

The authors wish to thank the CNPQ for the master scholarship for the first author, the FAPEMA for the master scholarship for the second author and the PQ Research Grant for the third author.

## REFERENCES

- Collares-Pereira, M., RABL, A. (1979), "The Average Distribution of Solar Radiation - Correlations between Diffuse and Hemispherical and between Daily and Hourly Insolation Values", *Solar Energy*, **22**, 155-164.
- Duffie, J.A. and Beckman, W.A. (2013), *Solar Engineering of Thermal Process*, John Wiley & Sons, NJ.
- He, Y.L., Xiao, J., Cheng, Z.D., Tao, Y.B. (2011), "A MCRT and FVM coupled simulation method for energy conversion process in parabolic trough solar collector", *Renewable Energy*, **36**, 976-985.
- Jeter, S.M., Jarrar, D.I., Moustafa, S.A.(1983), "Geometrical effects on the performance of trough collectors", *Solar Energy*, **30**, 109-113.
- Jeter, S.M. (1986), "Calculation of the concentrated flux density distribution in parabolic trough collectors by a semifinite formulation", *Solar Energy*, **37**, 335-345.
- Kalogirou, S.A. (2004), "Environmental benefits of domestic solar energy systems", *Energy Conversion and Management*, **45**, 3075–3092.
- Kalogirou, S.A. (2004), "Solar thermal collectors and applications", *Progress in Energy and Combustion Science*, **30**, 231-295.
- Liu, B.Y.H., Jordan, R.C. (1960), "The Interrelationship and Characteristic Distribution of Direct, Diffuse and Total Solar Radiation", *Solar Energy*, **4**(3), 1-19.
- Lovegrove, K. and Stein W. (2012), *Concentrating solar power technology – principles, developments and applications*, Woodhead Publishing, CB.